Journal of Zhejiang University SCIENCE A
ISSN 1673-565X (Print); ISSN 1862-1775 (Online)
www.zju.edu.cn/jzus; www.springerlink.com
E-mail: jzus@zju.edu.cn

# Simulation of dual transponder carrier ranging measurements*

Xiang-yu ZHAO†, Xiao-jun JIN†‡, Zhong-he JIN

(*Department of Information Science and Electronic Engineering, Zhejiang University, Hangzhou 310027, China*)

†E-mail: {zhaoxy, axemaster}@zju.edu.cn

Received Nov. 19, 2008; Revision accepted Feb. 20, 2009; Crosschecked Aug. 31, 2009

**Abstract:** The most dominant error source for microwave ranging is the frequency instability of the oscillator that generates the carrier phase signal. The oscillator noise is very difficult to filter due to its extremely low frequency. A dual transponder carrier ranging method can effectively minimize the oscillator noise by combing the reference phase and the to-and-fro measurement phase from the same single oscillator. This method does not require an accurate time tagging system, since it extracts phases on the same satellite. This paper analyzes the dual transponder carrier ranging system by simulation of the phase measurements with comprehensive error models. Both frequency domain and time domain noise transfer characteristics were simulated to compare them with dual one-way ranging. The simulation results in the two domains conformed to each other and demonstrated that a high level of accuracy can also be achieved by use of the dual transponder carrier ranging system, with relatively simple instruments.

**Key words:** Dual transponder carrier ranging, Dual one-way ranging, Oscillator noise, Transfer characteristic
**doi:**10.1631/jzus.A0820802 **Document code:** A **CLC number:** TN927; V566

## INTRODUCTION

Recently micro satellite formation flying has been an important field of space research, which completes cooperative work that cannot be accomplished by a single traditional satellite. Measuring the inter-satellite distance with high accuracy has been a key technology in formation flying. In military fields such as interferometric synthetic aperture radar (INSAR) and gravity gradient recovery, the accuracy of inter-satellite ranging has a great effect on ground altitude measuring, ground slow-motion target detection, and gravity field analysis (Bryant, 2003).

The earliest way of measuring the distance between satellites using a carrier wave was to count the number of carrier phases in one-way flight time. The accuracy of this method mainly depends on the stability of the oscillator that generates the carrier. Dual one-way ranging minimizes the oscillator noise effect by combining two one-way range measurements. The drifts of the two opposite carriers flying between satellites have equal magnitude but reverse direction. Thus, most oscillator drift error is eliminated when adding the two carrier phases together. The Gravity Recovery and Climate Experiment (GRACE) mission uses this method to measure changes in the range between two spacecrafts with an accuracy approaching 1 μm (Bertiger *et al.*, 2003). The twin GRACE satellites were launched into a 500-km orbit from Plesetsk cosmodrome, Russia on March 17, 2002. Both GRACE satellites were equipped with the following instruments (Davis *et al.*, 1999): K-band ranging system (KBR), accelerometer (ACC), GPS space receiver (GPS), and ultra stable oscillator (USO). KBR transmits and receives the dual-band K-band (24 GHz) and Ka-band (32 GHz) microwave signals. The four phases measured at the twin satellites in both frequency bands are combined to obtain range measurements without a long-time oscillator error or a first-order ionosphere error.

In one-way ranging, the phase shift between the measurement phase and the reference phase are generated by different oscillators at different times, including frequency fluctuations due to the two

‡ Corresponding author
* Project (No. NCET-06-051) supported by the Program for New Century Excellent Talents in University, China

oscillators' instability. In dual one-way ranging, the two one-way phase shifts are added together to make the measurement phase compare with the reference phase generated from the same oscillator. Accordingly, the phase differences become the phase relativities at different times while the time interval is the flight time of the carrier between the satellites. Thus, the long time oscillator error whose period is longer than the flight time is eliminated. Based on the principle of minimization of the oscillator noise by a dual one-way system, we propose a new dual transponder system. The new system generates a measurement phase from one stable oscillator, which travels from one satellite to the other. The measurement phase is then coherently transferred by the other satellite and then comes back to the first satellite, where it is subtracted from the reference phase. Since this system extracts the phase from the same oscillator, it can also remove the effect of the long time oscillator error (Zucca and Tavella, 2005). However, the dual transponder system brings in transfer noise due to the transfer instrument. And the Doppler noise of the dual transponder system is stronger than that of the dual one-way system for it doubles the flight time of the carrier. If it is proven that the dual transponder system achieves a high level of accuracy similar to that of the dual one-way system, there are several reasons for choosing the dual transponder system in practical applications. The dual one-way system needs an accurate time tagging system to synchronize the twin satellites as it samples phase shifts from different satellites simultaneously, while the dual transponder system does not rely on a time tagging system because it derives phase information from one satellite. Thus the dual transponder system does not need GPS or other complicated instruments to calibrate the time-tag precisely between satellites. On the other hand, since the range error is in proportion to the carrier frequency offset between the twin satellites in a dual one-way system (Kim and Tapley, 2005), the frequency offset is extremely small, i.e., 0.5 MHz in the K band carrier, which increases the difficulty in manufacturing the horn and microwave assembly. In the dual transponder system, the carrier frequency offset is irrelevant to the range error due to the elimination of the time-tag error (Kim and Tapley, 2005). As a result the frequency offset may increase to 200 MHz in the S band carrier, which makes the development for microwave assembly quite simple. The method used in the dual transponder system to eliminate the long-time drift is similar to the technique proposed for the Laser Interferometer Space Antenna (LISA) project, which uses highly stabilized laser light in an interferometer arrangement (Bender, 2000). The difference is the carrier frequency, which is a microwave frequency with a high offset in the two directions in the dual transponder system, much lower than the optical frequency in the LISA project. The simple instruments used, due to the low frequency, are compatible with the transponder equipment of the formation flying micro satellites, so as to complete the high precision range mission relatively easily in the satellite constellation.

To support the theory and structure of the dual transponder system, this paper simulates the noise characteristics in both the time domain and the frequency domain and predicts the accuracy of the range measurements considering all error sources including the oscillator error, system error, Doppler error, and multipath error. Simulation in the frequency domain establishes the analytical models of the structure and then computes and compares the effects on the range measurement of various noises transferred through the models. Simulation in the time domain computes every time the signals and the noises passing through physical models and analyzes the ranging accuracy of the dual transponder system. The simulation results in the frequency domain and time domain corroborate each other to prove that the dual transponder carrier ranging system is able to measure the changes in range between the satellites with a similarly high accuracy to that of the dual one-way system.

## THEORETICAL ANALYSIS

### Measurement equations

The structure of the dual transponder carrier ranging system is identical to that of the dual one-way ranging system where the two satellites both need to transmit and receive measurement signals (Kim and Tapley, 2002). The difference between the structures is that in the dual one-way system the two satellites transmit and receive the measurement signals simultaneously while in the dual transponder system they do that in sequence. Fig.1 shows the phase measurements of the dual transponder carrier ranging system.

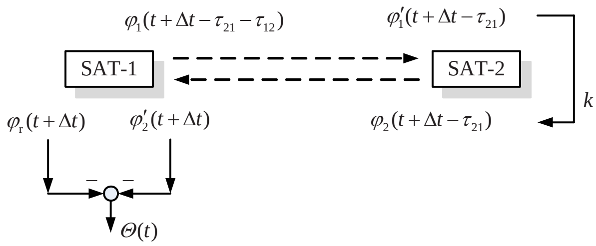


**Fig.1 Phase measurements of the dual transponder carrier ranging system**

The single-frequency carrier phase measurement at a nominal time $t$ can be modeled as follows:

$$\Theta(t)=\varphi_r(t+\Delta t)-\varphi_2'(t+\Delta t)+N+I+d+\varepsilon, \quad (1)$$

where phase $\Theta(t)$ is the difference between the reference phase of the 1st satellite, $\varphi_r(t+\Delta t)$, and the received phase from the 2nd satellite, $\varphi_2'(t+\Delta t)$. This measurement contains the integer ambiguity $N$, ionosphere phase shift $I$, phase shift due to other effects $d$, and measurement noise $\varepsilon$.

At the specified nominal time $t$, the single-frequency carrier received phase can be represented with the transmit phase as

$$\varphi_2'(t+\Delta t)=\varphi_2(t+\Delta t-\tau_{21}), \quad (2)$$

$$\varphi_1'(t+\Delta t-\tau_{21})=\varphi_1(t+\Delta t-\tau_{21}-\tau_{12}), \quad (3)$$

where $\tau_{21}$ is the time of flight from the 2nd satellite to the 1st satellite, and $\tau_{12}$ is the time of flight from the 1st satellite to the 2nd satellite. The 2nd satellite transfers the received phase from the 1st satellite, and the transfer maintains the synchronization between the input and output phase. The proportion of output phase to input phase is assumed to be $k$. Then the reference phase of the 1st satellite also synchronizes with the phase transmitted by the 1st satellite, and the scale factor is equal to that of the 2nd satellite.

$$\varphi_2(t+\Delta t-\tau_{21})=k\varphi_1'(t+\Delta t-\tau_{21}), \quad (4)$$

$$\varphi_r(t+\Delta t)=k\varphi_1(t+\Delta t). \quad (5)$$

Thus, the phase measurement can be substituted with the phase transmitted by the 1st satellite:

$$\begin{aligned}\Theta(t)=&k\varphi_1(t+\Delta t)-k\varphi_1(t+\Delta t-\tau_{21}-\tau_{12})\\&+N+I+d+\varepsilon.\end{aligned} \quad (6)$$

Each phase consists of the reference phase $\bar{\varphi}$, which corresponds to the constant reference frequency, and the phase error $\delta\varphi$ due to oscillator drift or frequency instability. The phase at $t+\Delta t$ and $t+\Delta t-\tau$ can be linearized around the phase at the nominal time $t$ with the rate of phase change $\dot{\bar{\varphi}}(t)$, which is equivalent to the constant nominal frequency $f$. The phase error can also be linearized in the same way, and the rate of phase error change, $\delta\dot{\varphi}(t)$, is equivalent to the frequency error, $\delta f(t)$. With these substitutions, the phase measurement can be represented as follows:

$$\Theta(t)=f_2(\tau_{21}+\tau_{12})+\delta f_2(t)(\tau_{21}+\tau_{12})+N+I+d+\varepsilon, \quad (7)$$

where $f_1$ is the frequency transmitted by the 1st satellite, $f_2$ is the frequency transmitted by the 2nd satellite, and $f_2=kf_1$ (Dean, 2003). The first term in the right-hand side of Eq.(7) represents the true phase measurement and the second term shows the errors due to the oscillator errors. The phase measurement of the dual one-way ranging system is expressed as (Kim and Tapley, 2003)

$$\begin{aligned}\Theta(t)=&f_1\tau_{12}+f_2\tau_{21}+(\delta f_1\tau_{12}+\delta f_2\tau_{21})\\&+(f_1-f_2)(\Delta t_1-\Delta t_2)+(\delta f_1-\delta f_2)(\Delta t_1-\Delta t_2)\\&+N+I+d+\varepsilon.\end{aligned} \quad (8)$$

Being the same as for the dual one-way ranging system, the oscillator error in the dual transponder carrier ranging system contains only the drift in the time of flight, while the long and medium wavelength oscillator noises have been removed effectively. But there is no time error between the nominal time and actual reception time, for the phases are derived at the same satellite.

The time of flights, $\tau_{21}$ and $\tau_{12}$, are slightly different. The phase measurement of the dual transponder system can be computed from the instantaneous inter-satellite range and Doppler correction range $\Delta\Theta_{DOP}$, with the assumption that the time of flights are equal to $\tau$.

$$f_1(\tau_{21}+\tau_{12}) \approx 2f_1\tau + \Delta\Theta_{\mathrm{DOP}}. \tag{9}$$

Convert the phase measurement to the range measurement by multiplication with an effective wavelength $\lambda$:

$$R(t) \equiv \lambda\Theta(t),\ \ \lambda = c/(kf_1). \tag{10}$$

All these substitutions yield the dual transponder range measurement $R(t)$ related to the instantaneous range $\rho(t)$:

$$R(t) = \rho(t) + \rho_{\mathrm{DOP}}(t) + \rho_{\mathrm{clk}}(t) + N + I + d + \varepsilon, \tag{11}$$

where $\rho_{\mathrm{DOP}}(t)$ is the range error due to Doppler shift, $\rho_{\mathrm{clk}}(t)$ is the range error due to the clock drift. The ionosphere phase shift $I$ can be approximated to be inversely proportional to the carrier frequency $f$. Suppose $f_1$ and $f_2$ are the dual transmit frequencies of the 1st satellite, and $\bar{F}_1$ and $\bar{F}_2$ are the dual transmit frequencies of the 2nd satellite. The dual-band combination algorithm is applied to obtain the ionosphere-free corrected range:

$$R = \frac{\bar{F}_1^2 R_1 - \bar{F}_2^2 R_2}{\bar{F}_1^2 - \bar{F}_2^2},\ \bar{F}_1 = \sqrt{k}\,f_1,\ \bar{F}_2 = \sqrt{k}\,f_2. \tag{12}$$

**Measurement error sources**

The error source of the dual transponder range measurement does not include the time-tag error, but contains the transfer noise due to the transfer instruments.

Only the oscillator noise or instability $\delta f(t)$ whose period is shorter than the time of flights affects the phase directly after dual transponder carrier ranging filtering. The oscillator noise characteristics depend on the specific oscillator, including $1/f$ noise, flicker noise, and integral white noise. In the higher frequency band above 0.01 Hz, the oscillator noise mainly exhibits itself as white noise and flicker noise, which do not have a large magnitude. The integral white noise predominates in the lower frequency band below 0.01 Hz and the noise magnitude grows higher as the frequency becomes lower. Thus, the dominant noise power lies in the low frequency band with a long jitter period. The dual transponder carrier ranging system has a strong suppression of low-frequency noise. The relationship between the phase measurement error and the oscillator noise is

$$\begin{aligned}\left|\frac{F[\delta\Theta(t)]}{F[\delta\varphi_1(t)]}\right| &= \left|\frac{F[\delta\varphi_1(t) - \delta\varphi_1(t-\tau_{21}-\tau_{12})]}{F[\delta\varphi_1(t)]}\right| \\ &= \left|1-\exp[-i2\pi f(\tau_{21}+\tau_{12})]\right| \\ &= 2\left|\sin[\pi f(\tau_{21}+\tau_{12})]\right|.\end{aligned} \tag{13}$$

As the frequency decreases to zero, theoretically the attenuation to oscillator noise grows to infinity. The error level of residual oscillator noise depends on the time of flight. A shorter separation distance is better for noise cancellation because it reduces the signal time of flight.

The Doppler range derivation is the difference between the carrier flight distance and the instantaneous inter-satellite distance, since the two satellites are moving. The instantaneous range correction term can be expressed as a function of the instantaneous range-rate, the velocity component along the line of sight vector, the time of flight difference, and the carrier frequency. Considering the variation in the satellites position at different times of transmission, transfer, and reception, the range correction is approximated by (Kim, 2000)

$$\rho_{\mathrm{MTP}} = \rho + \frac{1}{2}\dot{\rho}(\tau_{21}+\tau_{12}) + \frac{1}{2}\eta_2\Delta\tau, \tag{14}$$

where the instantaneous range $\rho$, the instantaneous range-rate $\dot{\rho}$, the 2nd satellite velocity component along the LOS vector $\eta_2$, and the time of flight difference $\Delta\tau$ are used. Therefore, it is necessary to quantify how accurately the individual parameters can be predicted. These accuracy levels are based on the estimation error using other measurements.

The system noise is due to the transfer instrument noise and receiver instrument noise. The major transfer noise comes from the phase-locked loop (PLL) used for frequency synthesis, including the phase detector noise, thermal noise from the loop filter, and phase noise of the oscillator. The mean value of receiver noise is mainly dependent on the distance between the two satellites or the signal-to-noise ratio (Wang *et al.*, 2006).

$$N_{\text{pll}} = N_{\text{pd\_ref}} + 10\log f_{\text{comp}} + 20\log(\varphi_{\text{out}} / \varphi_{\text{pd}}) + N_{\text{vcxo\_ref}} - 20\log(f / f_{\text{vcxo\_ref}}) + 20\log(\varphi_{\text{out}} / \varphi_{\text{vcxo}}) + 20\log(\sqrt{2}V_{\text{R}}\sqrt{4KTBR}\varphi_{\text{out}} / \varphi_{\text{R}}), \quad (15)$$

where $N_{\text{pll}}$ is the noise of the whole PLL, $N_{\text{pd\_ref}}$ the noise floor of the phase detector, $f_{\text{comp}}$ the detection frequency, $\varphi_{\text{out}}$ the output phase of the PLL, $\varphi_{\text{pd}}$ the output phase of the phase detector, $N_{\text{vcxo\_ref}}$ the noise floor of the voltage-controlled oscillator (VCXO), $f_{\text{vcxo\_ref}}$ the reference frequency of the VCXO, $\varphi_{\text{vcxo}}$ the output phase of the VCXO, $V_{\text{R}}$ the transfer function of the loop filter, $\varphi_{\text{R}}$ the output phase of the loop filter, $K$ the Boltzmann constant, $T$ the absolute temperature, $B$ the bandwidth of the loop filter, and $R$ the resistance of the loop filter.

The multipath error is due to the indirectly received signals, when the line of sight of two satellites is not perfectly aligned with the microwave antenna bore sight. This error may be a function of the satellite geometry and attitude control characteristics. According to a pessimistic estimation (Kim, 2000), the multipath range error may be given by

$$\Delta\rho = \sqrt{2}\varepsilon y\theta, \quad (16)$$

where $\Delta\rho$ is the range error by multipath, $\varepsilon$ is the amplitude reduction factor, $y$ is the reflection distance, and $\theta$ is the cone angle defined as the angle between the line of sight and spacecraft body fixed axis. Since the cone angle is computed from the yaw and pitch angle, it is important to control the attitude variation to within a specific level to minimize this error.

The transfer noise is mainly limited in a relatively narrow frequency band (Wang *et al.*, 2006); therefore, it can be attenuated by a carefully designed filter in post processing. In addition, the cone angle $\theta$ and the center of mass (CM) can also be determined accurately in a similar way in the dual one-way ranging, and the effect of multipath noise can be reduced by post-processing on the ground.

## SIMULATION PROCEDURE

The simulation proves the reasonableness of the dual transponder carrier ranging system in both the frequency and the time domains and predicts the range measurement accuracy. All the measurement error sources are added into the simulation to find out the impact of noise on the phase measurement after dual transponder carrier ranging filtering. In a spectral domain approach, the instrument error analyses are limited to certain types of error sources and assumptions, and the use of the time domain approach makes it possible to apply more extensive error models than by the analytic approach. Furthermore, the time-domain results allow us to validate the analytic and spectral analysis results (Kim and Tapley, 2003). To make a comparison with dual one-way ranging, the simulation calculates the results for the two ranging systems.

The first step of simulation in the frequency domain models the spectrums of all the noises. Then we derive the transfer function of each module in the dual transponder carrier ranging structure, such as signal transmission, signal transfer, space link, and signal reception. Finally, each noise is added to the appropriate location in the transfer function (de Gaudenzi *et al.*, 1993). The oscillator noise comes in front of the signal transmission, the Doppler error and the multipath error join the space link, and the system error is added to every module of signal transmission, transfer, and reception, according to practical circuit parameters, while the phase modulation error is involved in signal reception, as shown in Fig.2.

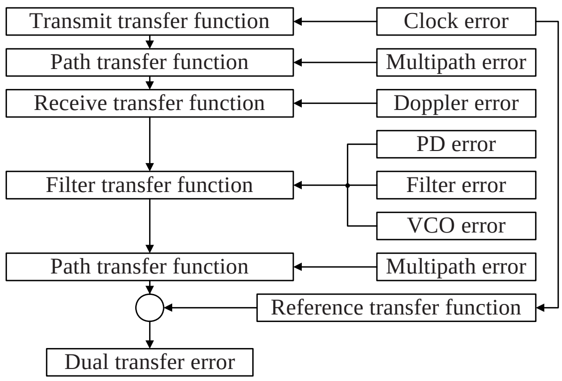


**Fig.2 Simulation steps in the frequency domain**

Simulation in the time domain first generates true positions for the two satellites at every moment. The time of signal generation and carrier flight is estimated accordingly. Then the reception phase and the reference phase are computed based on the oscillator characteristic and frequency changes (Harting, 1996). The phase measurement is derived from the subtraction of the reception phase from the reference phase, both of which are down converted by multiplication with the same local signal. The phase measurement is converted to range measurement by the use of Eq.(10). The dual frequency measurements are combined to obtain the ionosphere-free range in the meantime. In addition, the Doppler range correction is computed based on the orbit calculation. The last thing to do is to compare the range from the true model and the phase-derived conversion to find out the measurement error results, as shown in Fig.3.

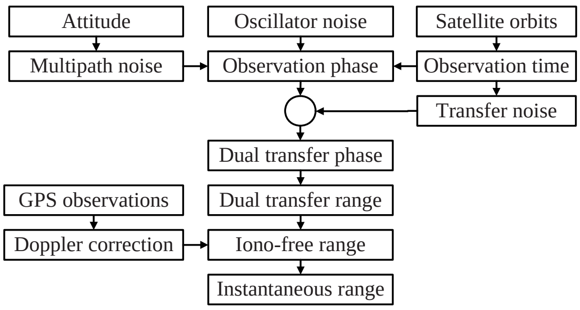


**Fig.3 Simulation steps in the time domain**

## SIMULATION CONFIGURATION

Table 1 describes the simulation data type and error model parameters.

**Table 1 Simulation parameter configuration**

| Parameter | Value/Description |
|---|---|
| Altitude (km) | 645 |
| Separation distance (km) | 239 |
| Eccentricity | 0.00 |
| Inclination (°) | 97 |
| Phase frequency bands | S (2 GHz), C (4 GHz) |
| Frequency offset (MHz) | 180 (S band), 360 (C band) |
| Data span (d) | 1 |
| Oscillator noise | Allan variance $2\times10^{-13}$ for 100 s |
| Multipath noise (μm/mrad attitude variation) | 0.15 |
| Doppler noise (μm) | 0.2 (for most dominant term) |
| Transfer noise (μm) | 3 (for most frequency bands) |

Orbit model parameters: The twin satellites travel on a low orbit with a separation of 239 km.

Measurement model parameters: Since there is no time-tag error, the carrier frequency can be set to a relatively low frequency band, say S band and C band (Kim and Tapley, 2005). The oscillator frequency remains the same as the dual one-way ranging.

Error model parameters: The oscillator error uses the same single-banded noise spectrum as the oscillator of the dual one-way satellites to compare the range structure filtering effect on the same oscillator model. The spectrum has a slope of 20 dB/decade under 0.01 Hz, and a slope of 10 dB/decade above 0.01 Hz (MacArthur and Posner, 1985).

The multipath error is configured with the parameters of a specific pica-satellite which can load the dual transponder carrier ranging system. The attitude control error level is 300 times that of the dual one-way satellites. But the pica-satellite has a small size, which is 1/20 that of the dual one-way satellites. With a pessimistic value −50 dB in the reduction factor, the impact of the multipath error on the range measurement is several times larger than on the dual one-way measurement.

The Doppler error level depends on the range-rate accuracy. On the basis of GPS measurements (Dunn *et al*., 2003), the accuracies of the range-rate, the velocity, and the time of flight are 0.1 mm/s, 1 cm/s, and $3\times10^{-11}$ s, respectively, which are independent of the frequency characteristics.

The transfer noise originates mainly from the system instruments. The noise floor of the phase detector is −216 dB/Hz, the noise floor of the VCO is −117 dB/Hz, and the reference frequency $f_{comp}$= 239 kHz. The PLL is equivalent to a low-pass filter of which the loop bandwidth is hundreds of kHz (Egan, 1990). The transfer function of the PLL maintains a constant in a frequency band below 10 Hz.

## SIMULATION RESULTS

The simulation takes the steps shown in Figs.2 and 3 with the parameters shown in Table 1 in both the frequency and the time domains. Compared with the dual one-way ranging measurements, the simulation results of dual transponder carrier ranging is shown as follows.

Fig.4a shows the single side-band phase noise spectrum of the oscillator. According to the spectrum in the time domain, the amplitude of the oscillator drift increases as time grows. Fig.4b illustrates the difference between the transfer function of the dual transponder carrier ranging and the dual one-way ranging. All the three curves exhibit strong suppression of long-time noise. The transfer function of the dual one-way ranging using GPS oscillator correction performs as a single straight line, where the magnitude decays linearly when the frequency decreases (Thomas, 1999). The transfer function of the dual one-way ranging using satellite USO oscillator correction remains the same as the previous one in the high frequency band above 0.01 Hz, but the attenuation at the low frequency below 0.01 Hz remains a constant much larger than the one using GPS oscillator correction. However, since the errors of dual transponder carrier ranging do not contain the time-tag error, the transfer function has nothing to do with the carrier frequency so that it remains a straight line similar to the one for dual one-way ranging using GPS correction. The residual oscillator error after dual transponder carrier ranging filtering is twice that achieved after dual one-way ranging because the time of flight of the dual transponder carrier ranging is doubled. As a result, the attenuation of dual transponder carrier ranging is 3 dB lower than that of dual one-way ranging. The conclusion is that the dual transponder carrier ranging performs much better than dual one-way ranging using USO correction in filtering the long-time oscillator noise, while the high-frequency performance is slightly worse than that of dual one-way ranging.

Fig.5 compares the power density spectrum of various noises in the dual transponder carrier ranging, where the true range change contains the effects of the gravity field and non-gravitational forces. The curve of the oscillator noise shows the result when the oscillator noise spectrum in Fig.4a passes through the dual transponder carrier ranging filter in Fig.4b. The error level of oscillator noise at low frequencies is about several micrometers, in particular below 1 μm at high frequencies above 0.01 Hz. The phase noise due to transfer circuits is included in system noise, and is independent of the frequency in a span of less than 0.1 Hz. The error level of system noise is close to 3 μm, which becomes the dominant error source in the 0.001~0.1 Hz frequency band. The multipath noise varies with the attitude control noise, of which the error level increases quite slowly with a frequency below 0.001 Hz, root mean square (rms) of 1 μm. But at the frequency above 0.001 Hz, the spectrum of multipath errors sharply decreases as the frequency grows. The error level of Doppler noise is relatively low among all the error sources, say rms of 0.2 μm.

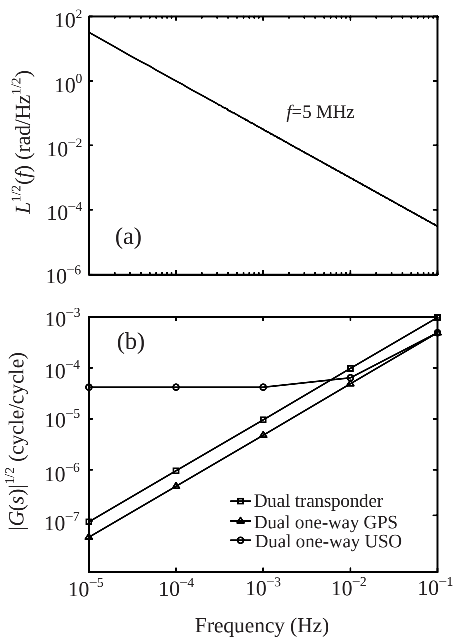


**Fig.4 (a) Single side-band phase noise spectrum of the oscillator; (b) Transfer function of ranging structure**

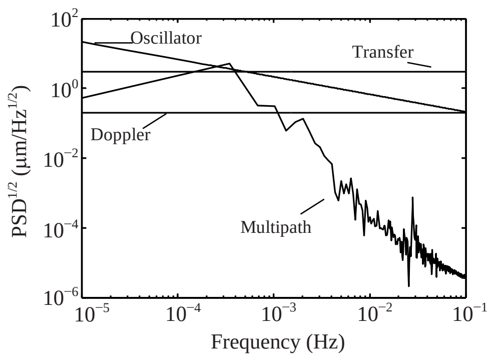


**Fig.5 Variable noise spectrum of dual transponder carrier ranging**

Fig.6 shows the power density spectrum of transfer noise. In the frequency band below 1 Hz, the power of the transfer noise remains 3 μm/Hz$^{1/2}$. There exists a peak value of 100 μm/Hz$^{1/2}$ at $10^4$ Hz when the noise power increases as the frequency grows. The strong transfer noise cannot be filtered by the dual transponder carrier ranging due to its high frequency and this would have a great impact on the accuracy of range measurement. But the high frequency noise can be easily removed using regular low-pass filters with a 10 Hz cutoff frequency (Thomas, 1989; Stephens and Thomas, 1995). Therefore, it is necessary to pass the phase measurements through low-pass filters to obtain transfer-noise-free range measurements.

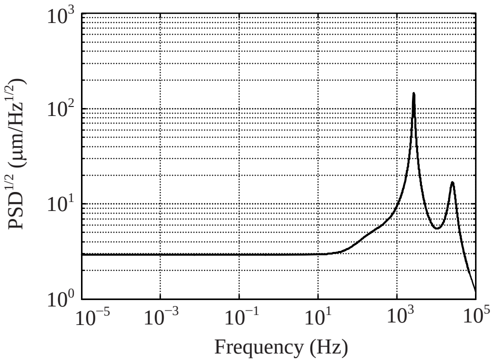


**Fig.6 Error spectrum of system transfer noise**

The results of simulation in the time domain are shown in Fig.7. Only oscillator noise effect is contained in the results. The time series of oscillator noise is expressed as range noise. Due to the strong long wavelength characteristic, the range noise drifts several millimeters during a time period of one day. Fig.7a illustrates the residual oscillator noise after ranging structure. Since both dual transponder carrier ranging and dual one-way ranging achieve a strong suppression of long-time oscillator noise, the results contain only the high frequency drifts at the low error level. The two range error results both exhibit strong periodic characteristics in a one-day period, as with the oscillator noise, which becomes the dominant error source of the range measurement error. The time of flight is about 1 ms so that the period of noise remaining in range measurement is shorter this time. The dual transponder carrier ranging and dual one-way ranging have similar accuracies, rms of the dual transponder carrier ranging is 0.94 μm, while rms of the dual one-way ranging is 0.53 μm. The error level of dual transponder carrier ranging is slightly larger due to its longer time in flight.

Fig.8 shows the power spectrum of the range error. At the highest frequency of 0.1 Hz, the error level is close to 0.1 μm/Hz$^{1/2}$. In comparison with the oscillator noise spectrum, the range error level in the low frequency band drops off significantly due to the strong suppression of the dual transponder carrier ranging, which conforms to the transfer function results in Fig.4b. At the lowest frequency of $10^{-5}$ Hz, the dual transponder carrier ranging performs better at a $10^4$ noise level than the dual one-way ranging at a $10^{10}$ noise level.

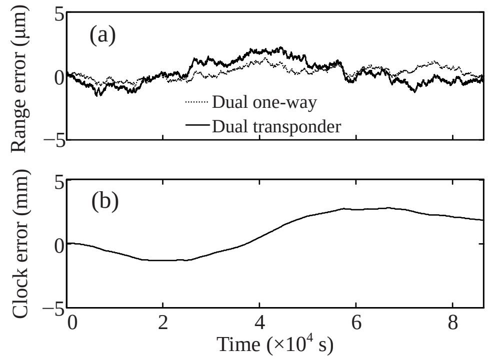


**Fig.7 Error time series of dual transponder carrier ranging.** (a) Range error; (b) Clock error

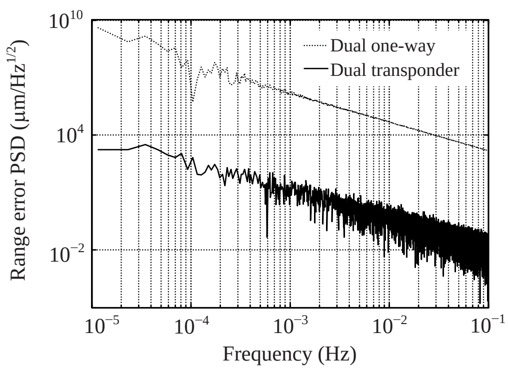


**Fig.8 Error spectrum of dual transponder carrier ranging**

Fig.9 shows the impact of the distance between satellites on the range measurement. As the distance increases, the range error level grows accordingly. This is because the distance variation changes the time of flight and also the filtering behavior of the dual transponder carrier ranging. According to Eq.(13), the attenuation on oscillator noise decreases as the flight time increases linearly. The residual noise frequency doubles when the time of flight doubles. As a result, the smaller the distance between the satellites, the lower the range error level and the higher the measurement accuracy.

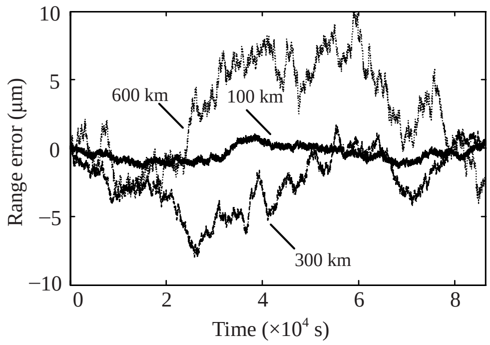


**Fig.9 Effect of the separation distance on the ranging accuracy**

## CONCLUSION

A new high-accuracy inter-satellite ranging system was described. Based on the dual transponder carrier ranging measurement equations, the theory has been derived to show how the dual transponder carrier ranging system removes most of the oscillator noise components effectively, without an accurate time tagging system. Both significant error sources contained in dual one-way ranging and new transfer noise brought by dual transponder carrier ranging were discussed. The simulation procedures to model and implement the noise were described. The simulation results demonstrated that the dual transponder carrier ranging system can achieve equal accuracy with the dual one-way ranging system, whereas the dual transponder system is more suitable in practical applications on account of its relatively simple instruments. The simulation tool was useful in implementing the dual transponder carrier ranging system in the subsequent signal processing algorithm.

## References

Bender, P., 2000. LISA Laser Interferometer Space Antenna: A Cornerstone Mission for the Observation of Gravitational Waves. System and Technology Study Report, ESA-SCI No. 11-65, Noordwijk, The Netherlands.

Bertiger, W., Dunn, C., Harris, I., Kruizinga, G., Romans, L., Watkins, M., Wu, S., 2003. Relative Time and Frequency Alignment between Two Low Earth Orbiters, GRACE. Proc. IEEE Int. Frequency Control Symp. and PDA Exhibition jointly with the 17th European Frequency and Time Forum, p.273-279. [doi:10.1109/FREQ.2003.1275101]

Bryant, L., 2003. Simulation Study of a Follow-on Gravity Mission to GRACE. MS Thesis, University of Colorado, Denver, USA.

Davis, E.S., Dunn, C.E., Stanton, R.H., Thomas, J.B., 1999. The GRACE Mission: Meeting the Technical Challenges. Paper IAF-99-B.2.05, International Astronautical Federation, Amsterdam, The Netherlands.

Dean, B., 2003. PLL Performance, Simulation and Design. National Semiconductor, Santa Clara, California. Available from http://www.national.com/appinfo/wireless/pll_designbook.html, p.88-150.

de Gaudenzi, R., Lijphart, E.E., Vassallo, E., 1993. A new high performance multipurpose satellite tracking system. *IEEE Trans. Aero. Electron. Syst.*, **29**(1):27-43. [doi:10.1109/7.249111]

Dunn, C., Bertiger, W., Bar-Sever, Y., Desai, S., Haines, B., Kuang, D., Franklin, G., Harris, I., Kruizinga, G., Meehan, T., *et al*., 2003. Application challenge: instrument of GRACE GPS augments gravity. *GPS World*, **14**(2):16-28.

Egan, W.F., 1990. Modeling phase noise in frequency dividers. *IEEE Trans. Ultrason. Ferr. Freq. Control*, **37**(4):307-315. [doi:10.1109/58.56498]

Harting, A., 1996. Considering clock errors in numerical simulations. *IEEE Trans. Instrum. Meas.*, **45**(3):715-720. [doi:10.1109/19.494587]

Kim, J., 2000. Simulation Study of a Low-Low Satellite-to-Satellite Tracking Mission. PhD Thesis, University of Texas at Austin, Austin, USA.

Kim, J., Tapley, B.D., 2002. Error analysis of a low-low satellite-to-satellite tracking mission. *J. Guid. Control Dynam.*, **25**(6):1100-1106. [doi:10.2514/2.4989]

Kim, J., Tapley, B.D., 2003. Simulation of dual one-way ranging measurements. *J. Space. Rock.*, **40**(3):419-425. [doi:10.2514/2.3962]

Kim, J., Tapley, B.D., 2005. Optimal frequency configuration for dual one-way ranging systems. *J. Space. Rock.*, **42**(4):749-751. [doi:10.2514/1.9974]

MacArthur, J.L., Posner, A.S., 1985. Satellite-to-satellite range-rate measurement. *IEEE Trans. Geosci. Remote Sensing*, **23**(4):517-523. [doi:10.1109/TGRS.1985.289443]

Stephens, S.A., Thomas, J.B., 1995. Controlled-root formulation for digital phase-locked loops. *IEEE Trans. Aero. Electron. Syst.*, **31**(1):78-95. [doi:10.1109/7.366295]

Thomas, J.B., 1989. An Analysis of Digital Phase-Locked Loops. JPL Publication 89-2, Pasadena, CA.

Thomas, J.B., 1999. An Analysis of Gravity-field Estimation Based on Inter-satellite Dual-1-way Biased Ranging. JPL Publication 98-15, Pasadena, CA.

Wang, C.H., Yu, F.X., Jin, Z.H., Zheng, Y.M., Zhao, X.Y., 2006. Research on noise of TT&C transponder for pico-satellites. *Syst. Eng. Electron.*, **28**(12):1514-1517 (in Chinese).

Zucca, C., Tavella, P., 2005. The clock model and its relationship with the Allan and related variances. *IEEE Trans. Ultrason. Ferr. Freq. Control*, **52**(2):289-296. [doi:10.1109/TUFFC.2005.1406554]